LA-UR-95- 2636

CONF-950846--21

Los Alamos National Laboratory is operated by the University of California for the United States Department of Energy under contract W-7405-ENG-36

TITLE: ORIENTATION-DEPENDENT SHOCK RESPONSE OF EXPLOSIVE CRYSTALS

AUTHOR: Jerry J. Dick, DX-10, LANL
Los Alamos, NM 87545

SUBMITTED TO: 1995 APS Topical Conference on "Shock Compression of Condensed Matter"
August 13-18, 1995 - Seattle, WA

Los Alamos
Los Alamos National Laboratory
Los Alamos, New Mexico 87545

DISCLAIMER

ORIENTATION-DEPENDENT SHOCK RESPONSE OF EXPLOSIVE CRYSTALS *

J. J. DICK

Group DX-1, MS P952, Los Alamos National Laboratory, Los Alamos, New Mexico 87545 USA

Some orientations of PETN crystals have anomalously high shock initiation sensitivity around 4 to 5 GPa. Results of a series of laser interferometry experiments at 4.2 GPa show that this is associated with an elastic-plastic, two-wave structure with large elastic precursors. Implications for the initiation mechanism in single crystals is discussed. Initial work on beta phase, monoclinic HMX is also described.

INTRODUCTION

Anomalous luminescent emission and initiation of detonation have been observed for two orientations of single crystals of pentaerythritol tetranitrate (PETN) in shock experiments near 4 GPa.(1) The crystals were more sensitive at 4.2 GPa than at 8.5 Gpa. From the data available it was not clear what was responsible for this anomaly. In addition to the sensitivity anomaly observed in wedge experiments, there was an unusual intermediate velocity transition between the initial shock velocity and the final detonation velocity in a wedge experiment on a [110] crystal. After consideration of these results it seemed that measuring time-resolved histories at several thicknesses through the initiation regime would be very helpful in clarifying the nature of the anomaly. Therefore a series of measurements of particle vs time at several thicknesses through the initiation regime was undertaken using velocity interferometry. The results are reported here. The results indicate that the anomaly is associated with separated elastic and plastic waves with large elastic precursors. In addition to the [110] experiments, experiments were performed at 4.2 GPa on [100] and [001] orientations as well. The records show orientation dependence in accord with previous luminescent experiments and a model of orientation dependence of shock sensitivity based on steric hindrance to shear.(2,1) Interferometry experiments were performed on [110] crystals at stresses ranging from 4.0 to 10.5 GPa in order to look at the variation in material response from the anomalous regime to the higher stress regime. The records show a continuous variation from one type of history to another. At higher stresses with a single shock, the initiating flow peaks further behind the shock wave. This results in slower shock growth at 6 and 7.2 GPa than at 4 to 5 GPa.

EXPERIMENTAL TECHNIQUE

PETN crystals were subjected to shock using a light-gas gun facility. Particle velocity vs time histories were recorded at the PETN/PMMA window interface using a velocity interferometer. Projectiles made of 2024 aluminum were impacted on Kel-F (polytrifluorochloroethylene) discs 50 mm in diameter and 5 mm thick. The PETN crystals were mounted on the aluminum-coated, Kel-F disc with a silicone elastomer. The crystals had typical lateral dimensions of 15 mm.

The measurement system used was a dual, push-pull, VISAR system.(3) The dual VISAR with different fringe constants removes ambiguity in determining the particle-velocity jump at the shock when extra fringes must be added. The light was transported from the argon-ion laser to the target and thence to the interferometer table with fiber optics.

EXPERIMENTAL RESULTS

In previous work(1) anomalous detonation was observed in a [110] PETN crystal in a wedge experiment at about 4.26 GPa. The run distance to detonation in wedge experiments was shorter at

*Work performed under the auspices of the U. S. Department of Energy

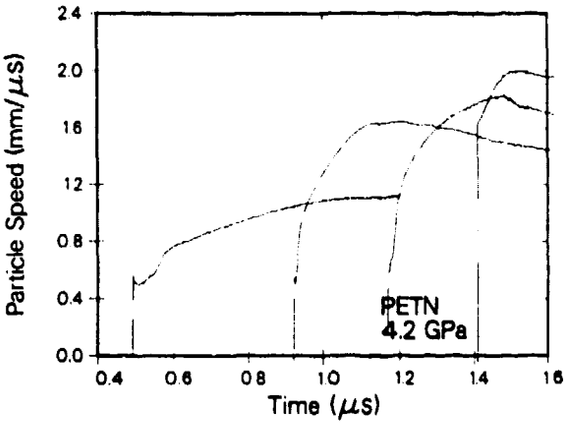

FIGURE 1. Particle vs time histories at the PETN/PMMA interface for a 4.15 GPa input shock at 1.825, 3.47, 4.44, and 5.55 mm PETN thicknesses of [110] orientation

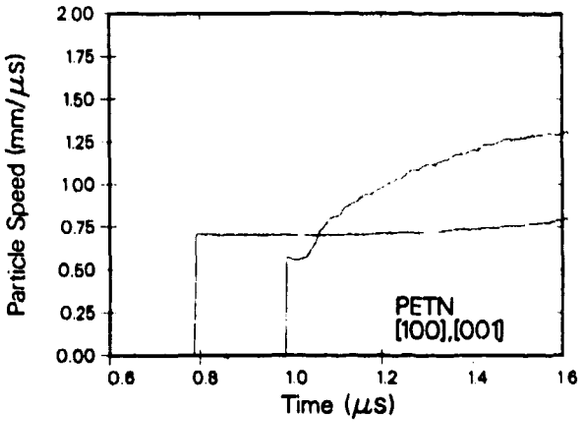

FIGURE 2. Particle vs time histories at the PETN/PMMA interface for a computed 4.15 GPa input shock strength for [001] and [100] orientations. The [001] crystal thickness was 3.79 mm and the [100] crystal thickness was 2.90 mm.

4.26 GPa than at 8.5 GPa. The run distance normally would increase and the sensitivity decrease with decreasing input shock stress. Furthermore, the run distance was the same at 4.2 Gpa and at 9.2 Gpa, a double-valued behavior. More experimental information was needed to clarify the behavior. In order to observe the behavior behind the leading shock wave, a series of four VISAR experiments was performed at 4.15±0.01 GPa on [110] crystals of different thicknesses in order to obtain particle vs time histories through the initiation regime. The first two with crystal thicknesses of 1.825, and 3.47 mm were in the region of constant initial shock velocity in the wedge experiment. The third at 4.44 mm thickness was at the onset of the intemediate velocity transition. The fourth experiment with a crystal thickness of 5.55 mm was in the region of the intermediate velocity transition. The particle velocity vs time histories obtained at the interface are shown in Fig. 1. It was unexpected to see a two-wave structure. In Ref.?? the leading wave was thought to be the bulk or plastic wave to the final shock states.

At 1.825 mm there is a large elastic shock followed by a plastic wave. The elastic wave amplitude is 2.74 Gpa in PETN. These precursor strengths are much larger than those seen for input shock strengths of 1.14 GPa. There the elastic precursor shock strength for [110] crystals was 1.0 GPa. Dependence of elastic precursor strength on input shock strength in [110] and [001] PETN crystals was noted in earlier work(4) for shock strengths up to 2.7 GPa. Elastic precursor strengths were as strong as 2.0 GPa after 5 mm of wave propagation in that work.

There is evidence of exothermic initiation chemistry causing increasing particle velocity immediately behind the plastic wave. The initiating flow accelerates the second wave so that it completely overtakes the elastic shock by about 4.6 mm causing the intermediate velocity transition. The detonation transition was at 6.6±0.2 mm in the wedge experiment.

In Fig. 2 particle velocity vs time histories for [001] and [100] orientations for the same input stress are displayed. For the [001] orientation an elastic-plastic, two-wave structure is displayed similar to that observed in [110] orientation. The elastic precursor strength is 3.15 GPa, larger than observed in [110] orientation. However, the initiating wave is weaker than in [110] at that thickness. In contrast, the [100] crystal displays a single wave to the final state followed by a nearly constant particle velocity indicative of essentially inert behavior.

DISCUSSION OF THE RESULTS

Elastic-Plastic Wave Structure

In the [110] and [001] orientations there is an elastic-plastic wave structure in the region of the

low-shock-stress sensitivity anomaly observed for [110] crystals. Initiation begins in or immediately behind the plastic wave. This is consistent with our model of steric hindrance to shear.(1,2) In the model the endothermic first step in explosive decomposition is chemical bond breaking in the sterically hindered shear flow in the plastic wave or shock. This leads to the exothermic decomposition steps on the way to initiation of detonation, especially at low stresses. Our previous geometric analysis of steric hindrance for rigid molecules found [110] and [001] orientations to be hindered and [100] and [101] orientations to be relatively unhindered. These results were corroborated by molecular mechanics analysis of deformable molecules for the cases considered, [100], [101], and [110]. For the [100] orientation there is a single wave with a flat following flow indicative of no initiation response is consistent with the minimal steric hindrance for this case. The small elastic precursor(2) has been overdriven by the plastic wave at this level of shock strength; i.e., the wave speed on the plastic Hugoniot is faster than the wave speed on the elastic Hugoniot for the input particle velocity of 0.616 mm/μs. Actually, the bulk wave velocity from the fit for PETN gives 3.83 mm/μs, whereas measured elastic wave velocities for this orientation were 3.42 and 3.73 mm/μs for input shock strengths of 1.14 and 1.56 GPa.(2) So the wave velocities are very close to the same value.

The two-wave structure explains another feature noted in earlier work.(1) From photodiode records of the luminescent emission it was inferred that there was an absorbing or dark zone behind the leading shock. This is consistent with the emission coming from the region of the plastic wave, not the leading elastic wave. The interpretation is that the peak in the photodiode signal and the subsequent fall in signal level is due to quenching of the emission in the crystal by the rarefaction from the free surface after arrival of the plastic wave. In Fig. 3 particle velocity records are shown of the elastic-plastic wave structure for [110] and [001] orientations. There are arrows on each record marking the time at which the photodiode peak would be based on data presented in our 1991 article.

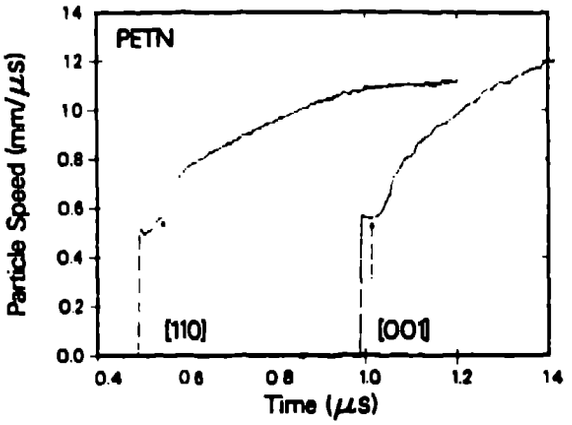

FIGURE 3. Particle vs time history at the PETN/PMMA interface for [110] and [001] crystals shocked to about 4.16 GPa. An elastic-plastic,two-wave structure is displayed by both records. The plastic wave is followed by increasing particle velocity due to exothermic initiation processes. In each case the arrow indicates the inferred position of the peak in emission as determined from a photdiode record in earlier work. The beginning of the fall in emission intensity coincides roughly with the beginning of the plastic wave. This indicates that the luminescent emission begins at the base of the plastic wave.

The photodiode records were obtained for crystal thicknesses different from those used in the VISAR experiments. For [110] orientation the photodiode record was for a crystal 2.79 mm thick vs 1.825 mm for the VISAR record. For [001] orientation the photodiode record was for a crystal 3.94 mm thick vs 3.79 mm for the VISAR record. The input shock stresses were were equal within 0.22 GPa for [110] orientation and within 0.11 for the [001] orientation. An analysis was performed in the position-time plane to determine the arrival time for the event associated with the photodiode peak at the sample thicknesses of the particle velocity records assuming a constant velocity for the disturbance. Account was taken of the particle velocity of the PETN/PMMA interface in the VISAR experiment and PETN free surface velocity in the emission experiment, but wave interactions were ignored. The disturbance arrival time t is given by:

$$t \quad t_0 \quad \frac{x_2}{u_1} \quad \frac{x_1}{u_1} \qquad (1)$$

where t_0 is the elastic wave transit time in the VISAR experiment, u_1 is the velocity of the

PETN/PMMA interface in the VISAR experiment, and U_{pk} is the apparent velocity of the photodiode peak from the photodiode experiment. The striking result as seen in Fig. 3 is that quenching of the emission begins as soon as the initial portion of the plastic wave arrives at the free surface, at least within the 10-20 ns accuracy of the analysis. This implies that the emission originates from the entire plastic wave not just behind it. It suggests that onset of emission coincides with the onset of sterically hindered shear. From time-resolved spectral measurements this emission was interpreted as due to excited electronic states of NO_2.(1) This raises the possibility that the emission is due to direct nonequilibrium excitation by the sterically hindered shear. As suggested in an earlier article(2) the endothermic first step in initiation may involve nonequilibrium excitation of molecules on a femtosecond time scale caused by a mechanical process, sterically hindered shear occuring in the plastic flow associated with the uniaxial strain in a plane shock. It is worth mentioning that the calculated homogeneous temperature rise at 4.2 GPa is about 100 °C. The peak in the spectral data corresponds to 5000 to 6000 K by Wien's law, an unreasonable heterogeneous temperature, much higher than detonation temperature. Furthermore the spectral curves do not fit those of a gray body with constant emissivity. Rather, the spectra have character of a chemiluminescent edge on the blue side. This result substantiates the previous conclusion that the observed emission is due to luminescence from excited electronic states.(1) While we consider the nature and timing of the emission to be evidence for a triboluminescent mechanism, the possibility that the sterically hindered shear causes vibronic uppumping followed by bond breaking, and that the electronic excited states are due to subsequent chemical reactions on a nanosecond time scale cannot be ruled out. Also, the dihedral angle changes by up to 60°, a much larger change than that caused by thermal motion. Ref. (5) suggests ways in which bond angle distortion can drastically change the electronic state of a molecule. Our molecular mechanics results indicated that significant bond angle strain occurred in PETN for the most hindered cases.(2)

HMX STUDIES

Work has begun on studying the unit cell of this monoclinic crystal. The space group is $P2_1/c$ Possible slip systems are being studied for relative steric hindrance for different possible shock orientations. Because of the reduced symmetry of the unit cell, there are many more cases to consider than for PETN. The known slip systems of anthracene and other molecular crystals of the same space group have been studied for possible guidance. The importance of twinning in deformation of HMX is another complication.(6,7) Crystals of 110 and 011 orientations in $P2_1/n$ have been cut into slabs in preparation for VISAR experiments.

REFERENCES

1. J. J. Dick, R. N. Mulford, W. J. Spencer, D. R. Pettit, E. Garcia, and D. C. Shaw, J. Appl. Phys. **70**, 3572 (1991).
2. J. J. Dick and J. P. Ritchie, J. Appl. Phys. **76**, 2726 (1994).
3. Willard F. Hemsing, Rev. Sci. Instrum. **50**, 73 (1979).
4. P. M. Halleck and Jerry Wackerle, J. Appl. Phys. **47**, 976 (1976).
5. J. J. Gilman, Phil. Mag. B **71**, 1057 (1995), in *High-Pressure Science and Technology-1993-Part 2, Amer. Inst. Phys. Conf. Proc. 309*, edited by S. C. Schmidt, J. W. Shaner, G. A. Samara, and M. Ross, p. 1349, New York, 1994, AIP Press.
6. S. J. P.Palmer and J. E. Field, Proc. R. Soc. Lond. A. **383**, 399 (1982).
7. R. W. Armstrong, H. L. Ammon, Z. Y. Du, W. L. Elban, and X. J. Zhang, in *Structure and Properties of Energetic Materials, MRS Symposium Proceedings, Vol. 296*, edited by D. H. Liebenberg, R. W. Armstrong, and J. J. Gilman, p 227, Pittsburgh, 1993, Mat Res. Soc. Press.